

## Chapter 4

### The $^{40}\text{Ca}$ experimental apparatus

There are a large number of factors that influence the design of an experimental system for trapping and cooling Ca atoms. In addition, there are necessarily strict requirements of such a system for use as an optical frequency standard in order to be able to obtain high levels of stability and accuracy. Engineering a simple, reliable and potentially compact system is also one of our goals. Here I will introduce the basic components of our system, which will be described in detail later in the chapter.

We need three major laser systems to fulfill the requirements of optical frequency metrology with microkelvin temperature Ca atoms (see Figure 4.1.) In  $^{40}\text{Ca}$ , the broad

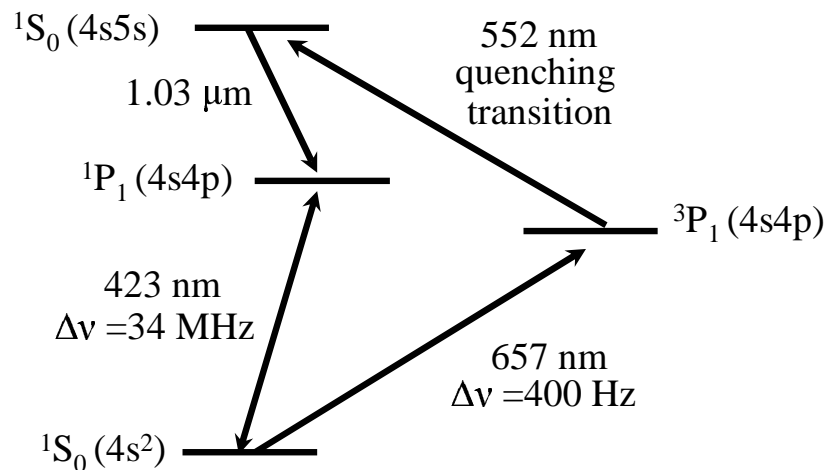


Figure 4.1: Energy level diagram for  $^{40}\text{Ca}$ , including cooling, clock and quenching transitions.

$(2\pi \cdot 34 \text{ MHz})$   $423 \text{ nm } ^1S_0 \rightarrow ^1P_1$  transition is ideal for basic broad-line Doppler cooling. With the use of optical and magnetic fields, we can trap and cool the atoms in a magneto-optic trap (MOT), extending the spectroscopic interrogation time of the atoms for frequency metrology. MOT technology is well developed for use with both alkali and alkaline-earth atoms. To create this 423 nm light, an infrared (IR) diode laser at 845 nm can be doubled in a nonlinear crystal. We wish to use the narrow  $(2\pi \cdot 400 \text{ Hz}$  natural linewidth)  $^1S_0 \rightarrow ^3P_1$  intercombination line at 657 nm as the clock transition for our standard. This wavelength is easily accessible by commercial diode lasers, which can be conveniently locked to an optical cavity. It is also relatively simple to coat these lasers (in house), greatly improving their performance. The necessary power for exciting these transitions could be easily attained with power amplifiers in the red and IR, commercially available at both wavelengths. After implementation, the entire red-blue setup filled only about four square meters of an optical table. A description of the initial system built by Oates *et al.* can be found in Reference [9].

The need for an additional laser system in second-stage quenched cooling creates a bit more complexity in the system, since diode-laser-based solutions were not available for the large amount of power needed at either possible quenching wavelength, 453 or 552 nm. The installation of a dye laser system was necessary to provide enough power for our 3-D experiments. At present we are working on designing a more compact and simple solid-state replacement.

#### 4.1 The 423 nm system

The  $^1S_0 \rightarrow ^1P_1$  cooling transition at 423 nm in neutral calcium has a natural linewidth of  $\Gamma/2\pi = 34 \text{ MHz}$ . This transition cycles photons 5 to 10 times faster than comparable cooling transitions used in alkali atoms. Although this cooling transition is not yet accessible with high power laser diodes, sufficient light at this wavelength can be made by doubling infrared (IR) light at 845 nm in a potassium niobate ( $\text{KNbO}_3$ ) crystal.

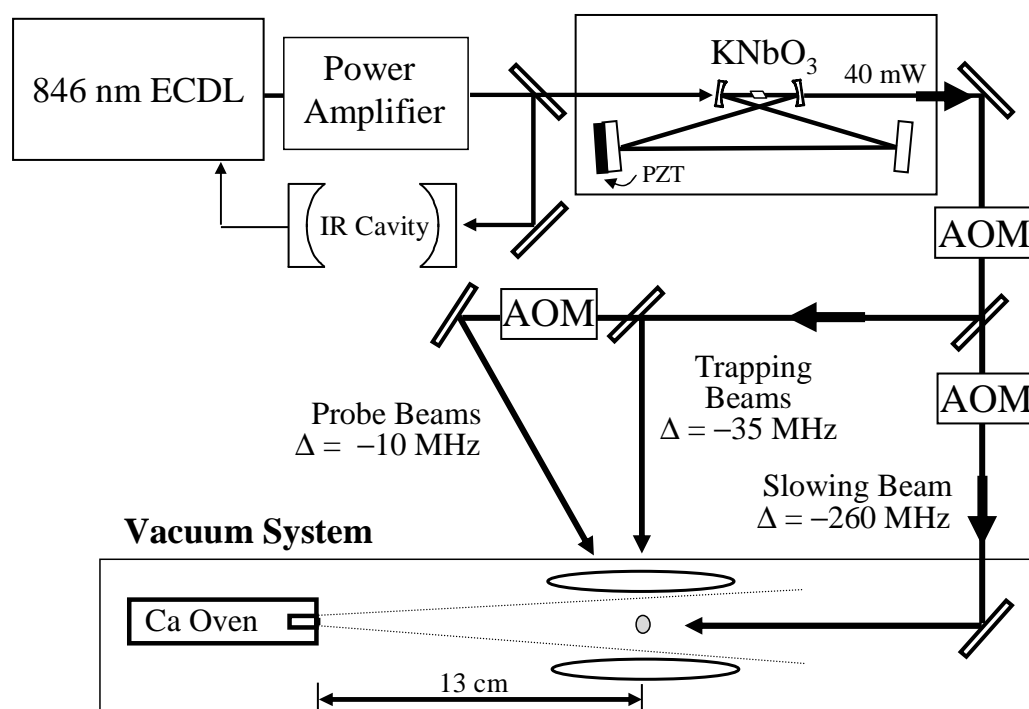


Figure 4.2: Schematic describing the laser and MOT system for trapping and cooling  $^{40}\text{Ca}$  atoms.

(See Figure 4.2 for 423 nm system diagram.) The diode laser is an SDL 5400 that we have AR coated to give it a reflectivity  $R \sim 10^{-3}$ . To increase the Q, which narrows the linewidth of the laser, we use an extended cavity diode laser (ECDL) configuration, with a cavity length of  $\sim 7$  cm. Our ECDL uses a grating (1800 grating lines/mm) to frequency select feedback to the laser diode and is aligned in the grazing incidence Littman-Metcalf configuration.[46] Figure 4.3 shows a schematic of the ECDL found in both the 845 nm and 657 nm maser lasers. Our IR diode laser produces about 20 mW

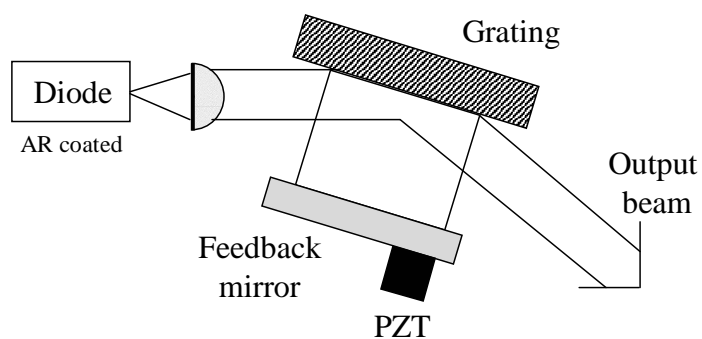


Figure 4.3: An ECDL in the Littman-Metcalf configuration. The PZT on the feedback mirror is used to tune the frequency of the diode laser by changing the frequency of light reflected off of the grating back in to the diode facet.

of 845 nm light that is sent into an SDL tapered amplifier that can produce almost 500 mW of light. A small fraction of this light is double-passed through an acousto-optic modulator (AOM) and coupled into an IR Fabry-Perot cavity, which is isolated from the environment in a vacuum can located inside a lead-foam-filled box. An AOM enables the tuning of the laser frequency near the cooling transition and bridges the gap between the cavity fringe (not tunable and drifting) and the Ca cooling transition frequency. The laser is locked to the cavity using -10 dBm sidebands written directly on the diode-laser current at 16 MHz for a Pound-Drever-Hall (PDH) lock [47] with feedback to a PZT that controls the horizontal tilt of the feedback mirror in the ECDL in order to correct the frequency of the laser. The majority of the light out of the amplifier is sent into the frequency-doubling system that was developed by Richard Fox and based on earlier

work by Carl Wieman. The input coupler to the bowtie-configuration cavity transmits 4.5 % in order to achieve a light build up factor of 30 in the 13 mm doubling cavity. The  $\text{KNbO}_3$  doubling crystal is at one focus of the cavity. The crystal is antireflection coated ( $R < 0.25$  % at 846 nm) and non-critically phase-matched for 423 nm at a temperature of  $-12^\circ\text{C}$ . To avoid condensation and freezing of water on the crystal face at this temperature, oxygen is blown over it and a bowl of desiccant rests in the cavity chamber. Using the same 16 MHz sidebands as for locking the IR cavity, reflected light from the front of the doubling cavity is used to servo and lock the frequency of the blue light. Total blue output power is  $\sim 40$  mW for  $\sim 200$  mW input. Although we have more available IR power from the power amplifier, higher power in the doubling cavity creates a less stable output, due to thermal effects in the crystal. We split this blue light into different beams for cooling, trapping, and probing, using AOMs both to create independent beams at different detunings and to have effective on/off switches between the light source and the atoms. AOMs are fast, efficient shutters, with a single blue AOM able to reduce the first-order light leakthrough by a factor of 1000 in only a few hundred nanoseconds. There are at least two AOMs in each blue beam in order to provide sufficient extinction of the light during clock spectroscopy. The blue light is intensity stabilized using a servo system that controls the rf power sent to the first blue AOM to  $\sim 0.1$  %. This greatly improves the overall stability of the measured fluorescence of the trapped and cooled atoms, and leads directly to improvements in our optical frequency metrology, as I will discuss in Chapter 6.

#### 4.1.1 The magneto-optic trap

We trap Ca atoms using a magneto-optic trap (MOT) as shown in Figure 4.4. We could completely copy the vapor cell MOT design first demonstrated for the alkali atoms, that loads atoms from a background vapor.[6] However, as mentioned before, one needs much higher temperatures for alkaline-earth atoms than for alkali atoms to

create a high enough vapor pressure to load a useful number of atoms, so hot trap windows must be made out of other substances more difficult to work with, such as sapphire. (Note: Although difficult, a vapor trap for Sr has been demonstrated by K. Vogel *et al.*[7].) Our MOT is loaded by means of a beam of thermal calcium atoms emanating from an oven reservoir that is heated to  $\sim 630$  K and located 13 cm from the trap. The reservoir is capped with a nozzle whose bore is 1 mm in diameter and 1 cm in length, which collimates the beam to an angle  $\theta = \sin^{-1}(\frac{1}{10})$ . The vacuum pressure inside the trapping region is  $< 10^{-7}$  Torr when the oven is hot, because Ca serves as a good getter of O<sub>2</sub>, N<sub>2</sub> and H<sub>2</sub>O. The atoms are caught in the MOT using three orthogonal, retroreflected, circularly-polarized blue beams in the typical  $\sigma^+ - \sigma^-$  configuration, detuned about 30 MHz to the red of resonance. We nominally collimate these to a 1 cm (1/e) beam size, focusing them slightly to account for some power loss due to the optics in the beam path. Since the magnetic gradient approximately scales with the width of the cooling transition we need to use a larger gradient than is typically used with alkali traps. We apply a magnetic gradient field of about 6 mT/cm (60 G/cm) using two anti-Helmholtz coils located outside the vacuum chamber. Each water-cooled coil is 10 cm in diameter with 100 turns. The coils are spaced 10 cm apart (the diameter of the MOT) and we run  $\sim 12.5$  Amps through them. It is not difficult for us to produce this gradient, but for atom cooling and spectroscopy we would often like to turn off the gradient quickly, which is difficult with the coils placed outside the metal trap apparatus, slowing the magnetic switching time due to eddy currents in the stainless steel vacuum chamber and the copper conflat gaskets.

Although our atomic beam loading method circumvents certain MOT design problems, we are still faced with the problem of loading a trap with a small capture velocity ( $\sim 20$  m/s) with an atomic beam that has a peak velocity of  $\sim 600$  m/s. In addition to the three cooling beams, we use a slowing beam detuned about 260 MHz below resonance in order to slow the atoms down to the velocity capture range of our MOT. (See

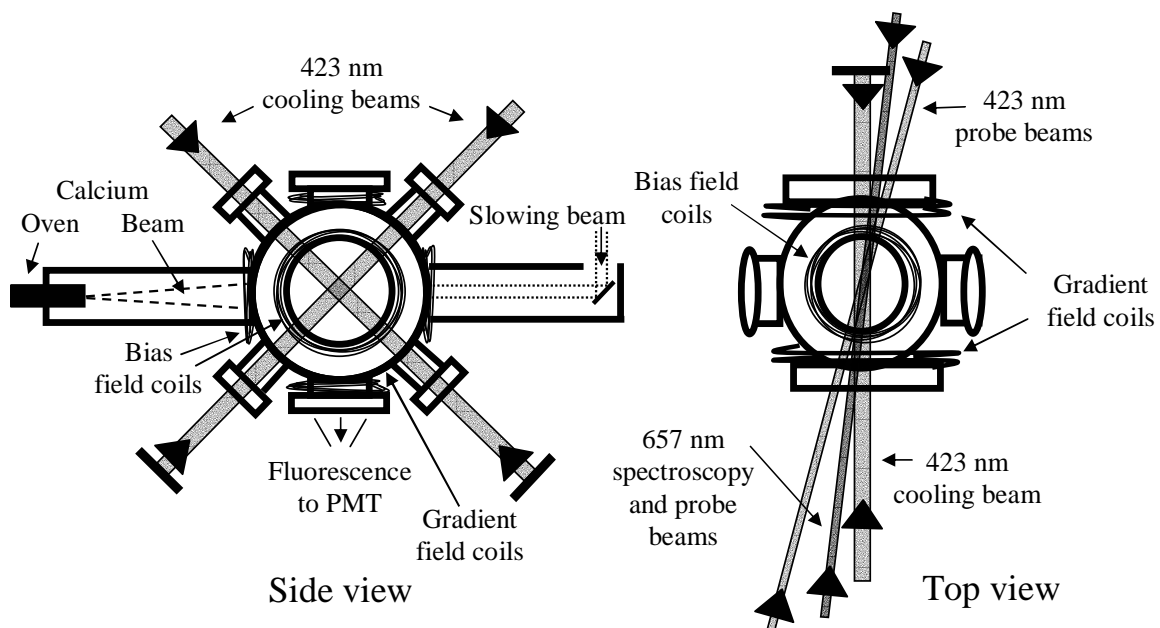
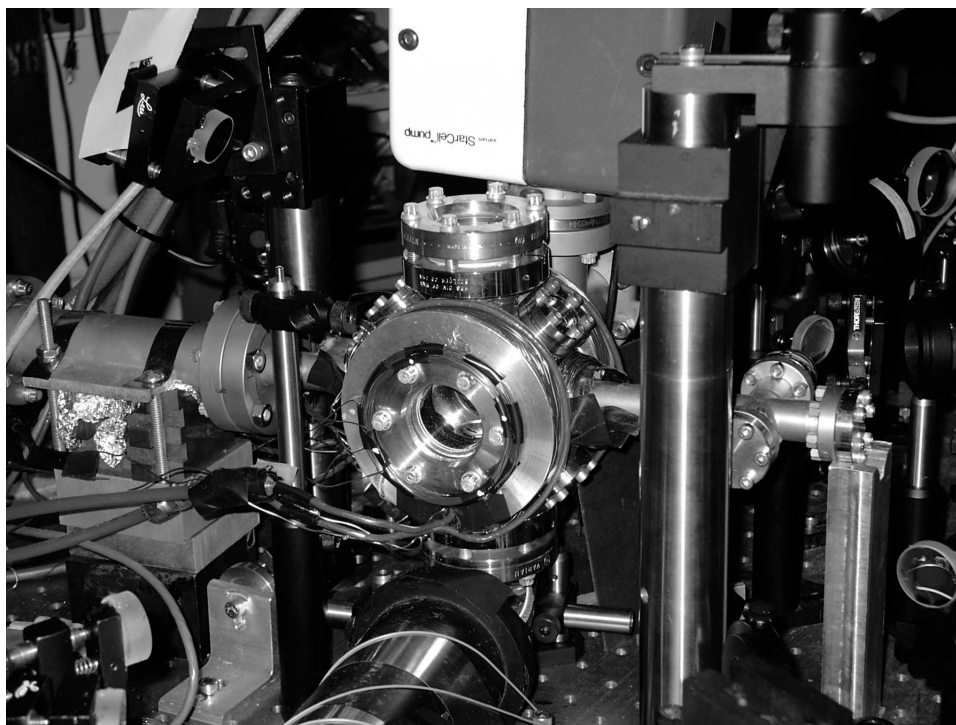


Figure 4.4: Photograph (upper) and schematic (lower) of magneto-optic trap (MOT), side view and top view.

Figure 4.4.) This beam is sent into the MOT antiparallel to the atomic beam and slows down those atoms that are resonant with that light ( $v \sim 100$  m/s), so that they too can be caught by the trapping beams. In an effort to slow down a larger range of velocities in order to load more atoms into the MOT, one can employ a Zeeman slower, which uses a magnetic field that changes spatially in order to compensate for the Doppler effect, keeping the atoms in resonance with the cooling light as they decelerate in the slowing beam.[8] Although we do not use a Zeeman slower, our apparatus in fact mimics this to some degree with its large trapping coils, creating a gradient field as the atoms travel towards the center of the trap. This increases the loading rate by a factor of 10, although we still catch  $< 0.1$  % of atoms from the beam. With this MOT system in place we are able to trap and cool about 5 million atoms to  $\sim 2$  mK during a 4-10 ms cooling cycle. The lifetime of the MOT in its present configuration is about 75 ms, limited by collisions of trapped atoms with hot atoms in the atomic beam as well as with atoms in the background gas.

## 4.2 The 657 nm system

For optimal clock performance, the 657 nm laser must have a linewidth significantly less than the natural linewidth of the clock transition,  $\sim 400$  Hz. The corresponding requirements on the 657 nm laser for narrow-line cooling are somewhat less stringent; the laser needs to have a linewidth of a few kHz in order to cool the atoms into the 100s of nanokelvin range. We fulfill these requirements using a 30 mW commercial diode laser (recently upgraded to 50 mW, Hitachi 6503) in the Littman ECDL configuration with a 10 cm extended cavity length. These lasers produce  $\sim 20$  mW (more recently  $\sim 30$  mW) of tunable, single frequency output power. We have temperature stabilized the baseplate of the laser cavity to prevent laser drifts and misalignment, greatly improving the overall stability of the laser lock. A 60 dB isolator just after the ECDL prevents feedback to the laser. A small fraction of this light ( $\sim 1$  mW) is double passed through

a 650 MHz AOM with 200 MHz of tuning range. This AOM is significant in the fact that it is used for tuning the laser relative to the reference cavity to which the laser is locked. This light passes through an electro-optic modulator (EOM) that writes small sidebands onto the light at 13.3 MHz, necessary for the PDH style locking technique we use. The modulated light is sent into a high finesse (linewidth = 9 kHz FWHM) Fabry-Perot cavity made of ultra-low expansion glass, whose end mirrors have 99.998 % reflectivity and have been attached via optical contact. Using light reflected from the cavity to generate the error signal, we lock the laser tightly to the cavity by sending fast frequency corrections to the laser current and correcting the slower frequency fluctuations with a PZT attached to the feedback mirror in the laser cavity. Additional

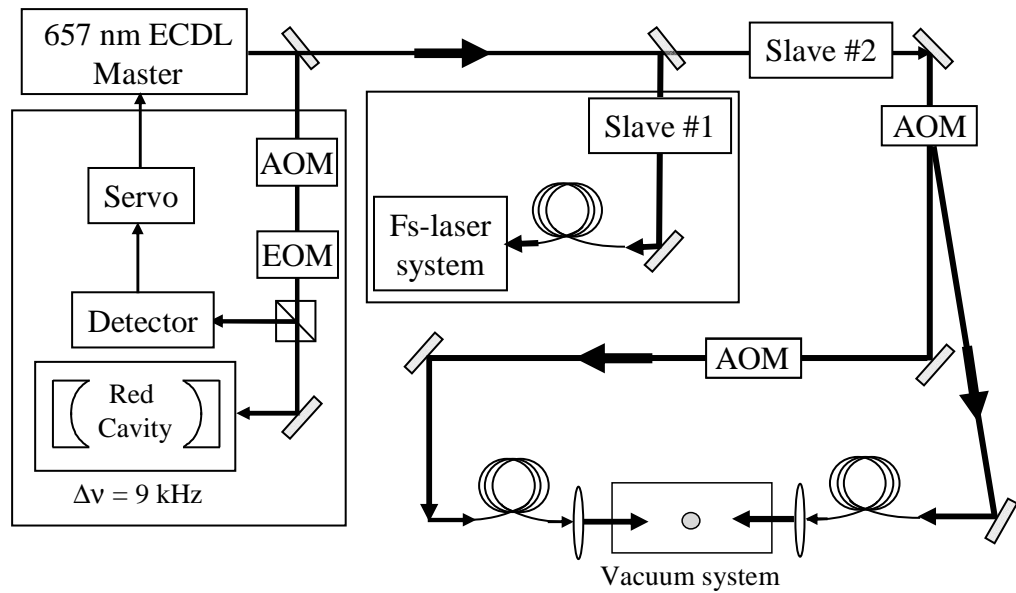


Figure 4.5: Schematic describing the laser system for spectroscopy on the narrow intercombination line in  $^{40}\text{Ca}$ . The largest slope corresponds to a drift  $< 15$  Hz/s.

noise can be written onto the laser if the Fabry-Perot cavity length fluctuates due to temperature variations and acoustic noise. To help isolate the high-finesse cavity from the environment, the cavity rests on O-ring spacers on a v-block of Invar, all residing inside a vacuum chamber. This chamber is surrounded by a larger aluminum box lined

with insulating and vibration-damping lead foam. The optical table on which the box, the laser systems and the MOT sits is on air legs (to help isolate the systems from vibrations) and is maintained level with three sensors referenced to the floor, actively controlling the height of the table. Recently, in order to further reduce cavity drifts (due to daily temperature fluctuations in the lab) we have added heater panels to the outside of this metal box and now actively servo the temperature of the box surrounding the cavity, reducing the cavity drift rate to less than 15 Hz/s. Figure 4.6 shows the drift rate of the locked laser system during a continuous 13.6 hour measurement using a femtosecond laser comb. With the laser system I have just described (see Figure 4.5) we have

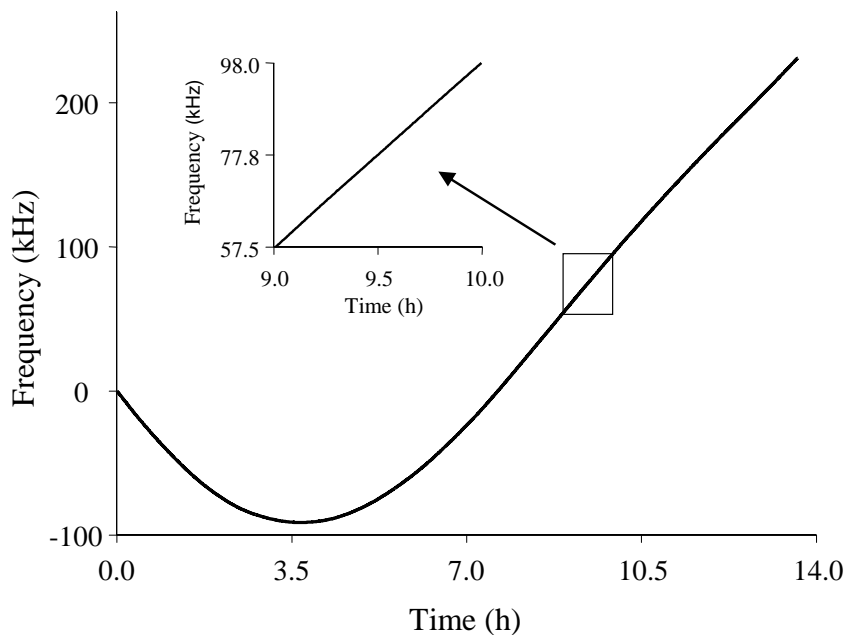


Figure 4.6: Measurement of the drift of the Fabry-Perot cavity using 657 nm laser light locked to the cavity and measured against a stabilized femtosecond laser system.

resolved features at and below the natural linewidth of the clock transition (see Figure 4.7) and recent experiments using ultracold atoms have shown that the fast-linewidth of the laser is well below 100 Hz (see discussion in Chapter 7.)

The majority of light out of the ECDL (10-15 mW) is sent to two slave lasers in

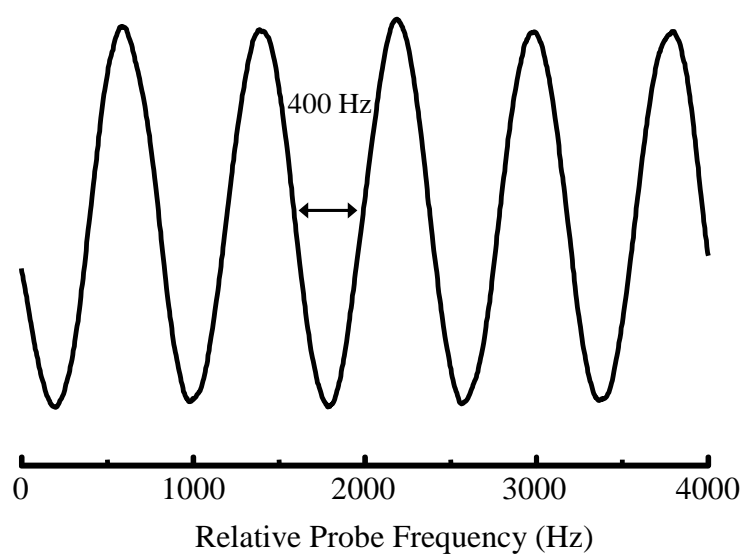


Figure 4.7: Experimental Bordé-Ramsey fringe pattern observed at the natural linewidth of the transition, 400 Hz, indicates the narrowness and stability of our 657 nm probe laser.

order to increase the available power for spectroscopy and cooling. In early phases of these experiments a semiconductor tapered amplifier (designed for 660 nm) was used to increase the power of the stable laser. It was then coupled into a fiber for spatial filtering. In the present setup, injection-locked laser diodes provide the amplification for frequency measurements and quenched-cooling experiments. (See Figure 4.5.) Typically a few milliwatts of master laser light was sufficient to cause the slave to preferentially lase at the frequency of the master laser diode, producing 40 mW output. (Note: We tested the fidelity of the slave laser frequency by shifting its frequency 80 MHz with an AOM and making a heterodyne measurement against light directly from the master laser.) We used AOMs to cut pulses out of the laser beam for probing and spectroscopy. A series of 2-3 AOMs were effective shutters, used to keep resonant light from reaching the atoms during the dark periods of the spectroscopy. In the injection-locked laser design, this light was then coupled into polarization-maintaining optical fibers using microscope objectives mounted on 3-D adjustable mounts. The fibers spatially filtered the light, which was recollimated with a lens on a 1-D mount after the fiber for easy adjustment/correction of the radius of curvature of the beam and then sent to the atoms in the MOT. After the AOM and fiber we have 10-15 mW of useful light.

### **4.3 The quenched-cooling laser systems**

The need for colder atoms required a quenched-cooling system, which added a further level of complexity to the Ca experiment. Not only did we need an additional red light source that would give at least 10 mW of power incident on the atoms, but we also needed a new laser system at 552 nm in order to be able to quench the red transition and make second-stage cooling possible (see Figure 4.1).

### 4.3.1 657 nm light for cooling

We needed approximately the same wavelength 657 nm light for cooling as we did for the clock transition spectroscopy, but we needed the frequencies for these two processes to be independently controlled. For 1-D quenched cooling this was accomplished with two counterpropagating linearly-polarized beams, previously used for Ramsey spectroscopy, see Figure 4.4, both beams used for cooling and a single beam used for probing. For 3-D trapping and cooling, we required more power, so we utilized the injection-locked red laser that had previously been used to send 657 nm light to the femtosecond laser comb for frequency measurements, adding an AOM to the system in order to control the timing of the red trap, and changed the polarization of the red beams to match those of the circularly-polarized blue MOT beams.

We tried a couple of different configurations of the 3-D red MOT beams, including using a single, retro-reflected beam passing through the chamber in all three orthogonal directions to make the red MOT. For this configuration, we made a single beam blue MOT and then overlapped this with the red beam using a dichroic beam combiner. We were able to trap atoms this way, but the alignment was very difficult and varied a great deal from day to day. For ease of alignment and optimization of the system we recently changed to a three-beam design with each blue beam retroreflected separately and each red beam independently overlapping one of the blue trapping beams to make a red MOT. This allowed the alignment of the red and blue traps to be independently controlled to help maximize the number of trapped atoms, as these beams are only overlapped a short distance before the trap. For many of the 3-D cooling results the red trap was in a two-beam configuration where the horizontal red beam was overlapped with the blue horizontal beam, and in the vertical plane there was only one retro-reflected beam of overlapped red and blue that travelled in two orthogonal directions and was retroreflected, as is shown in Figure 4.8. To make frequency measurements using

the ultracold atoms we needed the ability to send light to the frequency measurement system (see discussion in Chapter 6.) We freed up one injection-locked laser for the measurement by building an additional injection-locked laser devoted to providing light to the red trap.

### 4.3.2 552 nm light for quenching

To utilize the 552 nm quenching transition in Ca, we need a high power source of green light, as the quenching time is directly proportional to the quenching power. While the intercombination transition at 552 nm is weak, the linewidth is broadened to about 5 MHz due to the quick decay out of the  $^1S_0$  excited state to the  $^1P_1$  state. Thus the frequency stability requirements are not too stringent. For our first 1-D quenched cooling experiments we “borrowed” some green light from the Hg<sup>+</sup> dye laser of Jim Bergquist at NIST.[48] About 25 mW of 552 nm light was sent to our experiment via  $\sim$  180 meters of optical fiber. This beam was sent into the MOT at a slight angle to the blue and red horizontal trapping beams and retro-reflected, slightly focusing back through the trap. An AOM just after the fiber was used as a shutter and to carve out the necessary quenching pulses. For 3-D cooling and trapping we needed a fast cooling time compared to the time the atoms are lost from the trap by their thermal motion, and this necessitated an increase in green power. Moreover, we needed to have our own source of green light. To this end we were lucky enough to borrow an entire dye laser system from Carl Wieman. An argon-ion laser (Coherent innova 90) running between 5 and 6 Watts on all lines was used to pump circulating Rhodamine Chloride dye dissolved in ethylene glycol to produce tunable green light. The dye jet in the highly modified Spectra Physics laser is vertical and planer, and oriented at Brewster’s angle to the laser cavity. This cavity includes the usual optics to produce single frequency output and facilitate tuning over a broad range of wavelengths, including a thick etalon, a thin etalon, and a birefringent tuner. Small frequency adjustments are made with

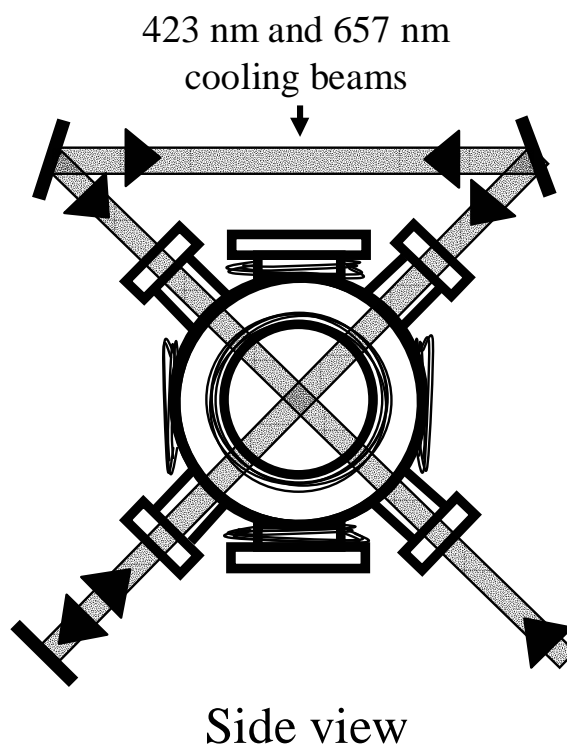


Figure 4.8: Beam geometry for 3-D quenched narrow-line laser cooling. The red and blue cooling beams are overlapped using dichroic red-blue beam combiners before they enter the MOT chamber, and then trace out the two vertical dimensions of the trap before being retroreflected. Another set of red and blue beams are also overlapped and retroreflected in the horizontal dimension (not shown).

galvanometer controlled Brewster plates, set as a pair rotating in opposite directions so as not to change the beam angle in the cavity. See Figure 4.9 for details.

We used the polarization spectroscopy method of Hänsch and Couillard to lock the laser to a confocal external cavity with an interior Brewster plate.[49] By sweeping the locked green light over many gigahertz, we were able to discern the transition frequency by watching the repump of excited ( $^3P_1$ ) calcium atoms back to the ground state. The drift of this cavity was suppressed by locking it to an  $I_2$  transition near the Ca 552 nm line, as shown in Figure 4.12.

We set up a conventional optical heterodyne saturation spectrometer [50] and resolved a 6 MHz wide hyperfine feature. Some 6 mW of light was picked off from the dye laser and an AOM shifted the frequency of that light 86 MHz so that, by using a 30 cm  $I_2$  cell and an EOM to frequency modulate the light at 12.9 MHz, we locked the laser to a saturated absorption feature in iodine. The narrow feature to which we locked was set on top of a Doppler-broadened background. The AOM directly before the  $I_2$  cell was modulated on and off and we used the difference between these two signals to remove the background and produce a flat baseline. The tunable frequency of the two AOMs helped bridge the gap of 43 MHz between the  $I_2$  line and the frequency needed to quench the  $^3P_1$  state in Ca. See Figure 4.10 for schematic diagram.

The dye laser system was located on a table in a separate room, adjacent to the Ca system, so this locked light was transferred to the Ca experiment via 10 m of optical fiber. In the initial 1-D experiments the green light was sent into the trap horizontally at a slight angle to the horizontal blue trapping beam and then retro-reflected. To quench in the 3-D trap, it was found that, due to power considerations and the circular polarization being used, it was only necessary to provide green light horizontally and in only one of the two vertical dimensions, as the circular polarization of the retroreflected green light (opposite to that of the red light) already allowed for all potential excitation paths. In this case the green was brought in horizontally, at a slight angle to the red and

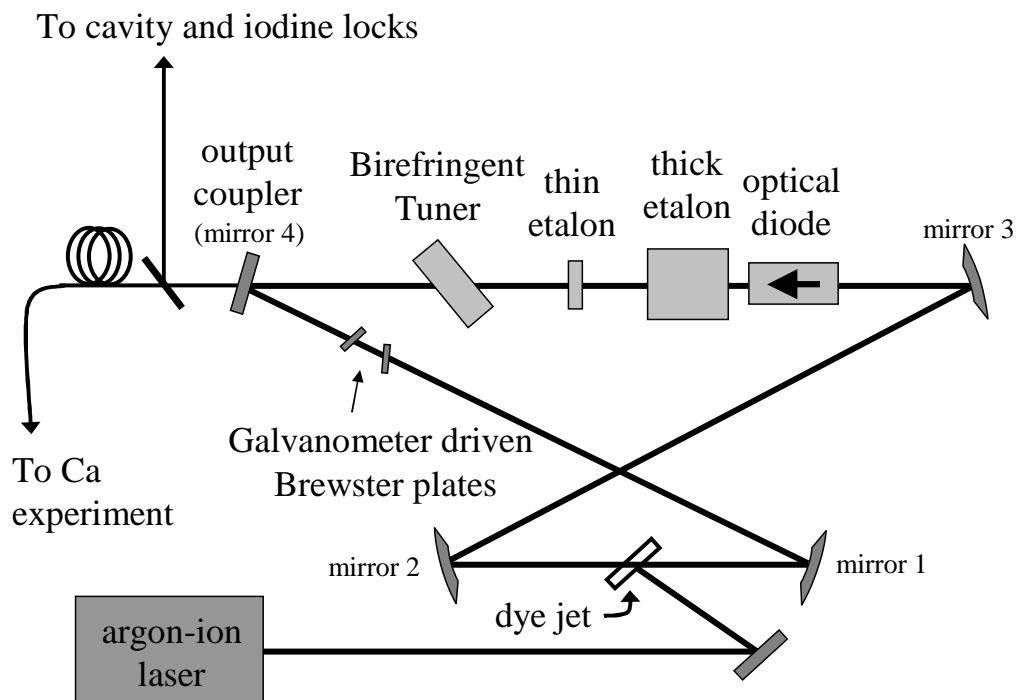


Figure 4.9: The dye laser system consists of an argon-ion pump laser and a circulating dye system. The dye laser produces about 300 mW of single frequency light, which can be easily tuned to our working wavelength of 552 nm.

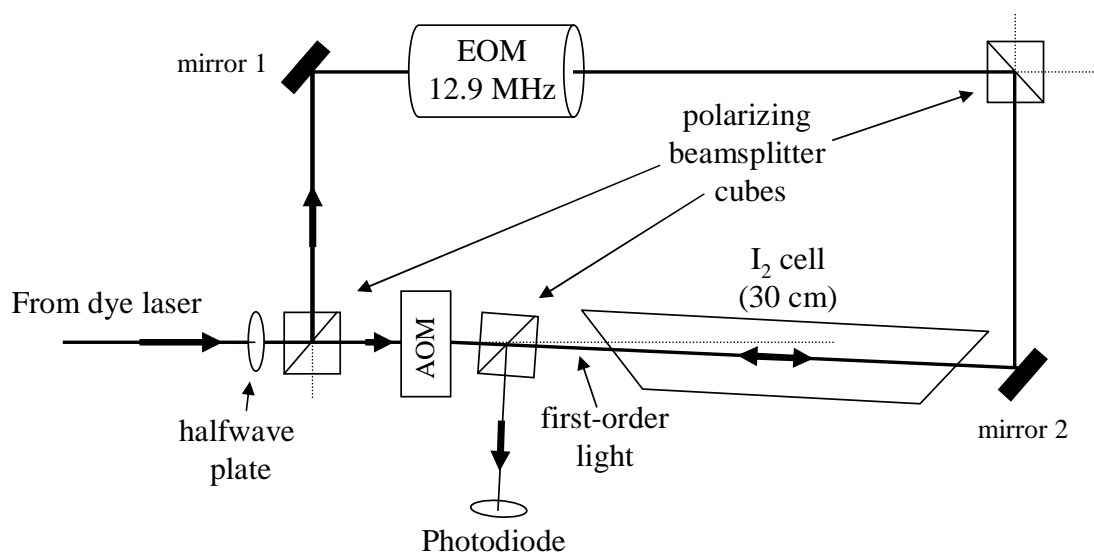


Figure 4.10: Schematic of the Iodine spectrometer.

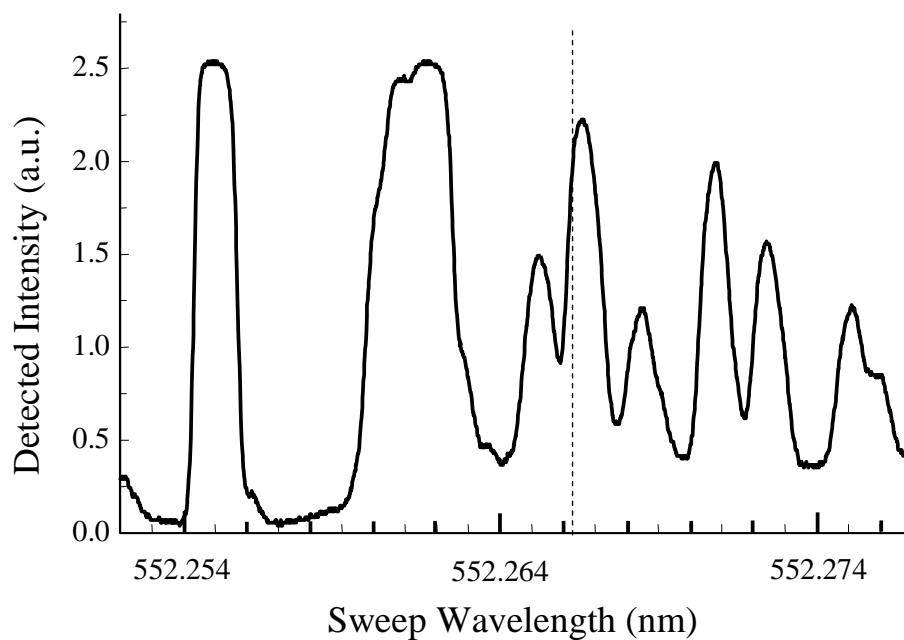


Figure 4.11: Sweep of Iodine spectrum showing the Doppler background near the relevant feature. Dotted line indicates approximate position of resonant frequency.

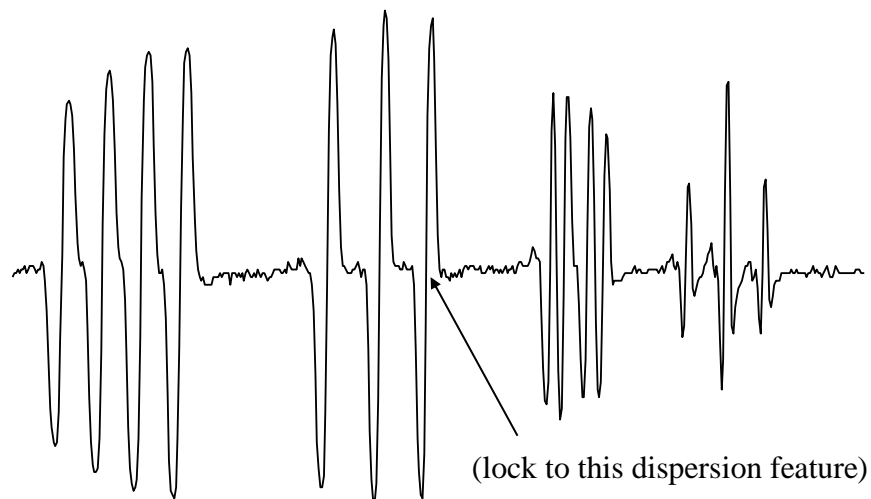


Figure 4.12: Smaller sweep of Iodine spectrum with AOM chopping shows the feature we use to lock frequency of the dye laser. (Sweep range  $\sim 500$  MHz.)

blue trapping beam, and then was reflected to also travel through the trap vertically, along the same path as one of the blue trap beams. This beam was then retroreflected back onto itself, see Figure 4.13.

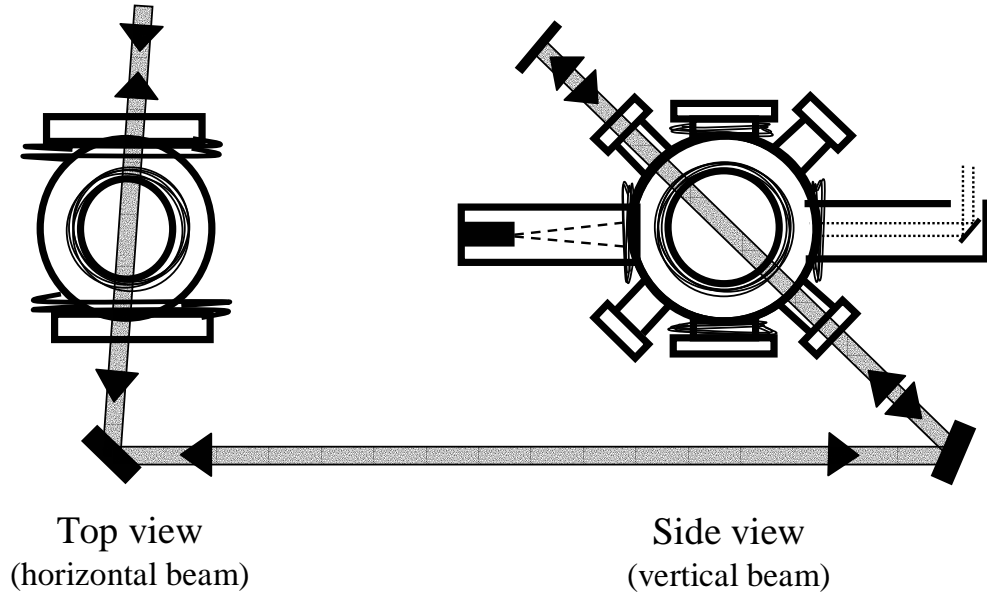


Figure 4.13: Schematic for the 2-D quenching beam geometry.

To be able to simultaneously achieve the correct cooling and quenching polarizations for all three colors ( $\sigma^+ - \sigma^-$  for red and blue beams, and the opposite circular polarization for the green beams), the blue  $\lambda/4$  wave plates in the initial MOT configuration were replaced with broadband versions. These were placed in the beam paths after the colors were combined, and also on the retro-reflection mirrors common to all beams.

## 4.4 Normalized shelving detection

### 4.4.1 423 nm detection

Sufficient signal-to-noise (S/N) in detecting the quantum state of the Ca atoms is not only necessary to allow us to probe the atoms and improve our system but is

essential for the creation of a frequency standard with good stability and accuracy. Perhaps the most intuitive way to probe the atoms in order to be able to measure the amount of atomic excitation induced by the 657 nm probe beams is to slowly sweep the frequency of the 657 nm probe laser and detect the fluorescence of the atoms as they decay from the  $^3P_1$  state, giving off red photons. This, however, is an inefficient approach since for our system one typically can only detect less than 1 in 1000 decays due to solid angle limitations and PMT detection efficiency. Also, the detection time will be proportional to the long lifetime of the level. An elegant solution to this problem is a detection scheme developed by Oates *et al.*[9] that was first demonstrated by H. Dehmelt for single trapped ion systems, which faced similar S/N limitations.[51, 52] They used a detection strategy based on collecting fluorescence from a strong cycling transition (also used for cooling) rather than attempt to detect the one photon from the decay of the ion from the excited state. (See Figure 4.14.) If the ion was in the ground state, shining near resonant cooling light on the ion would cycle it between the ground

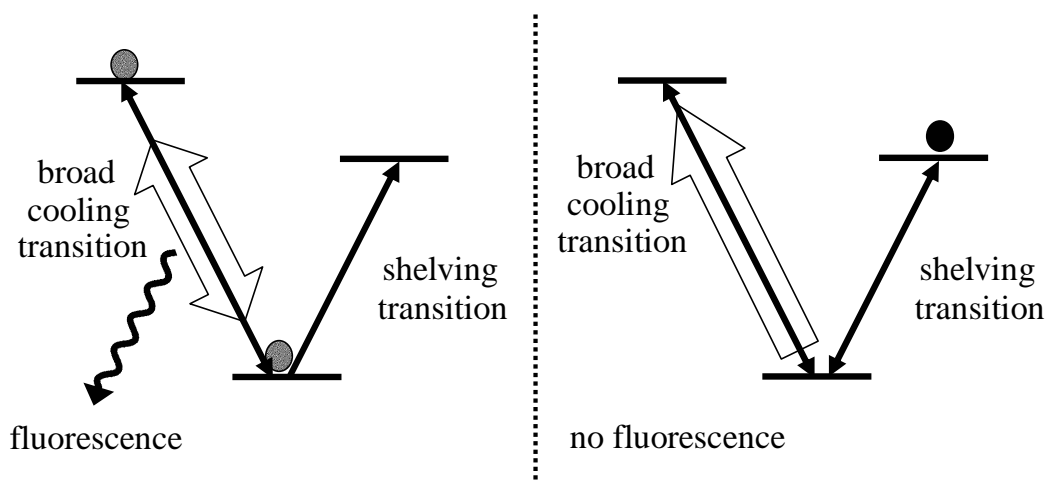


Figure 4.14: Energy level diagrams showing the process of shelving detection in the single-ion case. The left hand figure shows the case where the atom is not excited to the long-lived state. Then, light resonant with the broad transition will excite the atom and the atom will decay, giving off fluorescence. The right hand figure shows the case where the atom has been excited. Then, when the broad transition light is incident on the atom, the broad transition is not excited and there is no fluorescence to be detected.

and excited state, and through spontaneous emission many photons would be produced for fluorescence detection. If the ion was in the long-lived excited state, this cooling-transition light would have no effect on the ion and no fluorescence will be detected. In this way atomic excitation can be detected with essentially unit efficiency.

With some modification this “shelving detection” approach can work equally well for an atomic sample containing millions of atoms. For the Ca case, we use the fluorescence induced by two near-resonant pulses of blue light on the strong 423 nm transition to measure the number of atoms in the ground state (thereby allowing us to extrapolate the excited state population) using the measurement sequence depicted in Figure 4.15. First, when all the atoms have been cooled and are in the ground state, we use a slightly detuned pulse (detuned to the red  $\sim 10$  MHz so as not to cause significant heating of the atoms) of about 10- $\mu$ s duration to excite and cycle the atoms approximately 200 times between the ground state and the  $^1P_1$  state. The fluorescence detected will be proportional to the ground state population. This beam is incident on the atoms in the same direction as the horizontal blue cooling beam, but at a slight angle to that beam. In our system we use a lens within the vacuum system to collect the fluorescent light radiated from the atoms and transfer it to a photomultiplier tube (PMT). The lens subtends about 5 % of the  $4\pi$  steradians of fluorescence. The collected fluorescence is then stored as an electronic signal using a gated integrator. We then perform spectroscopy using the narrow 657 nm line, exciting some fraction of the atoms to the  $^3P_1$  state. Before these atoms decay (recall their 400- $\mu$ s lifetime), we measure the ground state population again with a second blue pulse and store this voltage using a second gated integrator. By dividing the second gated integrator signal by the first, we can determine the fraction of atoms in the excited  $^3P_1$  state. Moreover, due to this normalization the signal will be largely insensitive to fluctuations in atom number or blue-light intensity. By using this blue-fluorescence-based shelving detection scheme we achieve a S/N that is 20 times better than with detection using the 657 nm transition due to the increased

measured fluorescence and higher PMT efficiency (4 times higher for blue photons than red photons). This increase in S/N not only greatly improves the stability of the clock signal, but enables real-time detection of the spectroscopic signals, greatly accelerating experimental progress.

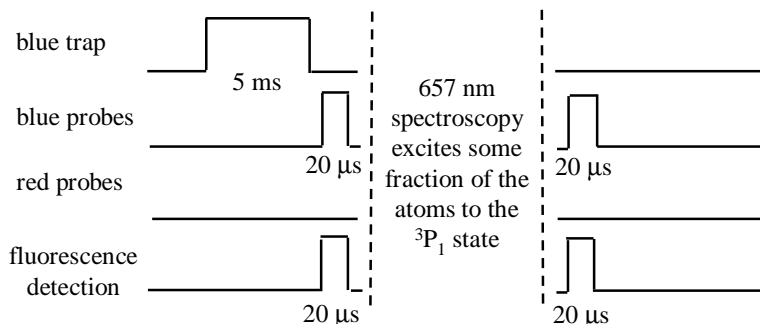


Figure 4.15: Timing diagram for normalized shelving detection.

#### 4.4.2 423 nm detection with quenching

For second-stage cooling the method of blue detection needed to be modified for two reasons. First, we could not use a blue normalization pulse after the second-stage cooling because the blue light would heat the atoms. Second, moving the blue probe pulse to just before the quenched-cooling sequence would make the detection system sensitive to atom number fluctuations in the second-stage cooling process. However, with the ability to quench the long-lived red transition quickly with green light, we were able to implement a slightly different scheme to retain the high S/N of the system. The basic change from the previous detection scheme is that the normalization pulse is moved from the beginning (before the quenched cooling) to the end, after all the cooling has taken place. (See Figure 4.16.) The new first blue detection pulse then measures the fluorescence of the now cold atoms remaining in the ground state after performing some red excitation pulse sequence or just a single red probe pulse. After that measurement the green light is pulsed on ( $\sim 150\text{-}\mu\text{s}$  duration) to send all the atoms back down to the

ground state. Then a second blue probe pulse measures the total atom fluorescence for normalization purposes. The only time delay between the two blue pulses is the green quenching pulse, which is significantly shorter than the time between the pulses if we were using the old scheme, which could be as much as 10 ms of red-green trapping and cooling time. The net result is that we can make measurements at the same S/N level as with the original shelving detection of the 2.4 mK atomic sample, but after significantly cooling the atoms.

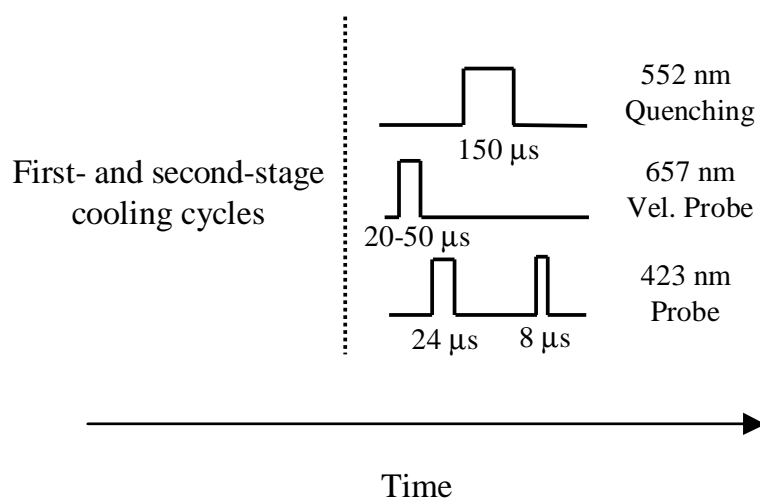


Figure 4.16: Timing diagram for normalized shelving detection with quenching. All detection occurs after the cooling cycles.